Pressure mediated structural transitions in bulk $EuTiO_3$

D. Bessas,[1,*] K. Glazyrin,[2,†] D. S. Ellis,[3] I. Kantor,[4] D. G. Merkel,[4] V. Cerantola,[5] V. Potapkin,[6] S. van Smaalen,[7] A. Q. R. Baron,[3] and R. P. Hermann[8]

[1]*Fundamental Aspects of Materials and Energy, Department of Radiation Science and Technology, Delft University of Technology, Mekelweg 15, 2629 JB Delft, The Netherlands.*[‡]
[2]*Deutsches Elektronen-Synchrotron, D-22607 Hamburg, Germany*
[3]*Materials Dynamics Laboratory, RIKEN Spring-8 Center, 1-1-1 Kouto, Sayo, Hyogo, 679-5148 Japan*
[4]*European Synchrotron Radiation Facility, F-38043, Grenoble, France*[§]
[5]*European Synchrotron Radiation Facility, F-38043 Grenoble, France.*
[6]*Institut für Mineralogie, Universität Münster, Corrensstr 24, D-48149 Münster, Germany*[¶]
[7]*Laboratory of Crystallography, University of Bayreuth, Universitaetsstrasse 30 D-95440 Bayreuth, Germany*
[8]*Materials Science and Technology Division, Oak Ridge National Laboratory, Oak Ridge, Tennessee 37831, USA*[¶]

The high pressure structural phase diagram of $EuTiO_3$ is revisited by means of single crystal X-ray diffraction at pressures below 30 GPa. We report a transition at about 3 GPa with a surprisingly small lattice distortion. At 23 GPa we have detected a yet unknown transition into a new orthorhombic phase (space group $Ibam$). Combining our observations on structures obtained on single crystals and polycrystalline samples with complementary methods such as electrical resistivity and nuclear forward scattering of synchrotron radiation measured on polycrystalline samples we address issues relevant to chemistry and disorder.

I. INTRODUCTION

The phase equilibrium in perovskites is very sensitive to slight variations of external parameters, and it is no surprise that changes of pressure and temperature produce effects similar in magnitude as chemical pressure, $i.e.$, the ionic radius of the ions involved in the structure, their concentration, the concentration of defects.

$SrTiO_3$ is one of the benchmark compounds with a perovskite structure highly appreciated for its electrical properties, $e.g.$, in varistors[1] and microwave filters[2]. $EuTiO_3$ is an incipient ferroelectric, similar to $SrTiO_3$. It hosts a magnetic cation and a magnetic transition to a G-type antiferromagnetic phase[3] occurs at about 5.5 K at ambient pressure. This magnetic state is found to be switchable by an electric field in strained films that exhibit a giant magnetoelectric coupling[4].

The phase diagram in $SrTiO_3$ is very well documented. At ambient pressure a structural transition from a cubic to a tetragonal structure[5] occurs at about 110 K. The pressure-temperature phase diagram in $SrTiO_3$ is well established up to 53 GPa[6]. Given the similarities in the high temperature structure, the volume of the unit cell, the bulk moduli of $SrTiO_3$ and $EuTiO_3$ it is reasonable to assume that similar phase transitions would be observed driven by similar contractions induced either by variation of temperature or pressure in $EuTiO_3$. It is, thus, attractive to study the phase equilibrium in $EuTiO_3$ under externally applied pressure and/or variable temperature.

The available literature on the structural phase equilibrium at ambient pressure in $EuTiO_3$ contains many controversies. For example, cubic, space group $Pm\bar{3}m$, symmetry of $EuTiO_3$ was long believed to be stable down to 4 K[7]. Indications for an antiferrodistortive phase transition to a tetragonal, space group $I4/mcm$, phase were reported with critical temperature varying between 200 and 287 K[8–12]. Goian $et\ al.$,[13] reported by means of electron diffraction a low temperature incomensurate phase which shows a treatment history dependent stuctural behaviour. Kennedy $et\ al.$,[14] used a combination of X-ray and neutron scattering as well as electric and magnetic measurements and attributed the observed discrepancies to the oxygen stoichiometry and defects. In a previous study[15] on purely Eu(II) containing polycrystalline $EuTiO_3$ indications of a structural transition were missing down to 10 K. Instead, Eu delocalization was observed and attributed to short-range coexistence of competing crystallographic phases with candidate space groups: $Imma$, $R\bar{3}c$ and $I4/mcm$.

The influence of stoichiometry and purity in the phase equilibrium of $EuTiO_3$ is clearly mentioned in several studies, $e.g.$, the effect of nitrogen substitution or oxygen content[16,17], hydride substitution[18], and presence of Eu^{3+} ions[19]. However, considering the experimental literature on $EuTiO_3$[3,8–11,14–18,20–23] only few studies have used methods sensitive to the valence state of the cations, $e.g.$, Mössbauer spectroscopy which is sensitive to Eu[15] and X-ray photoelectron spectroscopy which is sensitive to the valence state of both Eu and Ti[16,17].

The influence of pressure and temperature on $EuTiO_3$ was reported by Parisiades $et\ al.$,[20] utilizing X-ray powder diffraction. The authors used samples prepared in the same way as in Ref.[9]. At room temperature, a transition from the cubic phase (space group $Pm\bar{3}m$) to the tetragonal phase (space group $I4/mcm$) is indeed observed at about 3 GPa. However, only limited information on the structure is available in the study by Parisiades $et\ al.$,[20]. Access to diffraction data by single crystalline samples could shed more light on the intrinsic structural variations in $EuTiO_3$ under externally applied pressure, which could be related to other physical properties of the material.

In this study we report that single crystalline $EuTiO_3$ at 300 K exhibits two distinct structural phase transitions up to 30 GPa. At $3(1)$ GPa super-structure reflections to the $Pm\bar{3}m$ space group appear without any splitting of the main reflections. In good agreement with Ref.[20] this new structure can be indexed as a tetragonal phase (space group $I4/mcm$), and

is similar to the "pseudo-cubic" structure reported in Ref.[13]. At $8(1)$ GPa a splitting in the main reflections of the latter structure is observed. At higher pressure, $23(1)$ GPa, another transition to the $Ibam$ space group is observed. Moreover, we indicate that purely Eu(II) containing polycrystalline $EuTiO_3$ exhibits a single valence state up to 20 GPa and that the Eu magnetic ordering features are missing down to 20 K at 20 GPa.

II. METHODS

Both single crystals and polycrystalline samples have been used in this study in order to check the consistency of the crystallographic results at high pressure. For the same reason, we used two pressure transmitting media and the data was collected in two synchrotron radiation facilities.

The polycrystalline samples - used herein - are from the same batch as in Ref. [15], while the single crystals are from the same batch as in Ref. [12,24]. Both the polycrystalline samples as well as the small single crystals used here exhibited a simple structure without superlattice peaks at ambient conditions. Between the studies, the samples were stored at ambient conditions for about 3 years and show no sign of aging.

The data obtained by single crystals was collected at the station P02.2/PETRAIII (wavelength: 0.2893 Å). The beamsize was 3 μm x 8 μm. We used single crystals with approximate dimensions 15 μm x 15 μm x 10 μm loaded into a sample chamber of a diamond anvil cell equiped with diamonds of 300 μm culet size. The pressure transmitting medium used for the single crystal loading was Ne. Notably, the data obtained in a well prepared single crystal experiment is usually free from micro-strains, $e.g.$, inter-grain strain broadened X-ray diffraction profiles. The X-ray diffraction patterns were obtained by rotating the sample ± 28 deg around the ω axis in steps of 0.5 deg. The acquired data was analyzed and refined using the software packages: DIOPTAS[25], FIT2D [26], CRYSALIS PRO [27] and JANA2006[28].

The structural phase equilibrium under externally applied pressure was further studied by diffraction of synchrotron radiation on polycrystalline samples at room temperature at station P02.2/PETRAIII (wavelength: 0.2898 Å), see Supplementary Material, and ID27/ESRF (wavelength: 0.3738 Å), see Fig. 2. All diffraction data was collected using a 2D detector, $i.e.$, PE XRD1621 and Mar165, respectively. The diffraction data was refined with JANA2006[28]. The pressure media used for the polycrystalline sample loading were: a methanol - ethanol mixture (4:1) and Ne for the data obtained at PETRAIII and ESRF, respectively. In both cases a diamond anvil cell with 200 μm diamond culet size and rhenium gaskets were used. By employing Ne as pressure transmitting medium we tried to minimize effects of deviatoric stresses in the samples under study. Notably, although Ne solidifies at about 5 GPa at 300 K the pressure gradients remain less than 1% even up to 50 GPa[29].

In order to compare the results obtained in this study with existing reference data[14] and to provide a benchmark for future studies, the charge carrier density in the polycrystalline samples is quantified using electrical resistivity measurements. The electrical resistivity data was measured between 5 and 300 K using the four probe method on a small rectangular parallelepiped piece of $EuTiO_3$ in 10 mbar He using the Quantum Design-Physical Properties Measurement System (QD-PPMS).

Moreover, ^{151}Eu Nuclear Forward Scattering[30] (NFS) measurements in polycrystalline $EuTiO_3$ were carried out at the beamline ID18/ESRF under externally applied pressure, up to 20 GPa, and the potential Eu magnetic ordering at low temperature, down to 20 K, was studied. The lifetime, $t_0 = 14.4$ ns, of the ^{151}Eu first excited state at 21.541 keV fits in the interbunch time spacing of 176 ns in the 16 bunch mode operation of ESRF. The ^{151}Eu natural isotopic abundance 47.8% is adequate to carry out NFS measurements without further isotopic enrichment. A diamond anvil cell with 500 μm diamond culet size and stainless steel gasket was located in a cryostat. The pressure medium was paraffin oil. The pressure was monitored before and after each actual measurement by measuring the fluorescence of a ruby close to the sample. An average pressure value and the corresponding error bars are provided.

III. RESULTS

A. Single crystal X-ray diffraction

A transition from a cubic symmetry (space group $Pm\bar{3}m$) to a tetragonal symmetry (space group $I4/mcm$) at about 3 GPa is identified in our data obtained by single crystals. This transition manifests through an appearance of new reflections which are forbidden in the $Pm\bar{3}m$ space group, see Supplementary Material. Similar to Ref.[13] we observe reflections with a wave vector of $(\frac{1}{2}\ \frac{1}{2}\ \frac{1}{2})$ in the $Pm\bar{3}m$ space group. Such reflections correspond to the $(2\ 1\ 1)_t$[39] set of reflections in the tetragonal symmetry (space group $I4/mcm$) with lattice parameters relation $a_{I4/mcm} = b_{I4/mcm} = \sqrt{2}a_{Pm\bar{3}m}$ and $c_{I4/mcm} = 2c_{Pm\bar{3}m}$. Unlike in Ref. [13], we could not detect any signal from an incommensurate phase.

The transition from the $Pm\bar{3}m$ space group to the $I4/mcm$ space group leads to formation of twins. This effect was reproduced in various sample loadings. The observation of twinning did not prevent us from conducting structural refinement and obtain good quality data at higher pressures [31]. The splitting of the main Bragg reflections in the tetragonal symmetry become obvious at about 8 GPa. Above 23 GPa a new transformation into an orthorhombic symmetry is identified which could be indexed using the $Ibma$ space group, see Fig. 1. Detailed tables with information on single crystal diffraction data refinement can be found in the Supplementary Material.

B. Powder X-ray diffraction

Characteristic X-ray diffraction patterns from polycrystalline samples as function of pressure with Q up to 5.5 Å^{-1} are recorded in this study. The observed powder rings are uni-

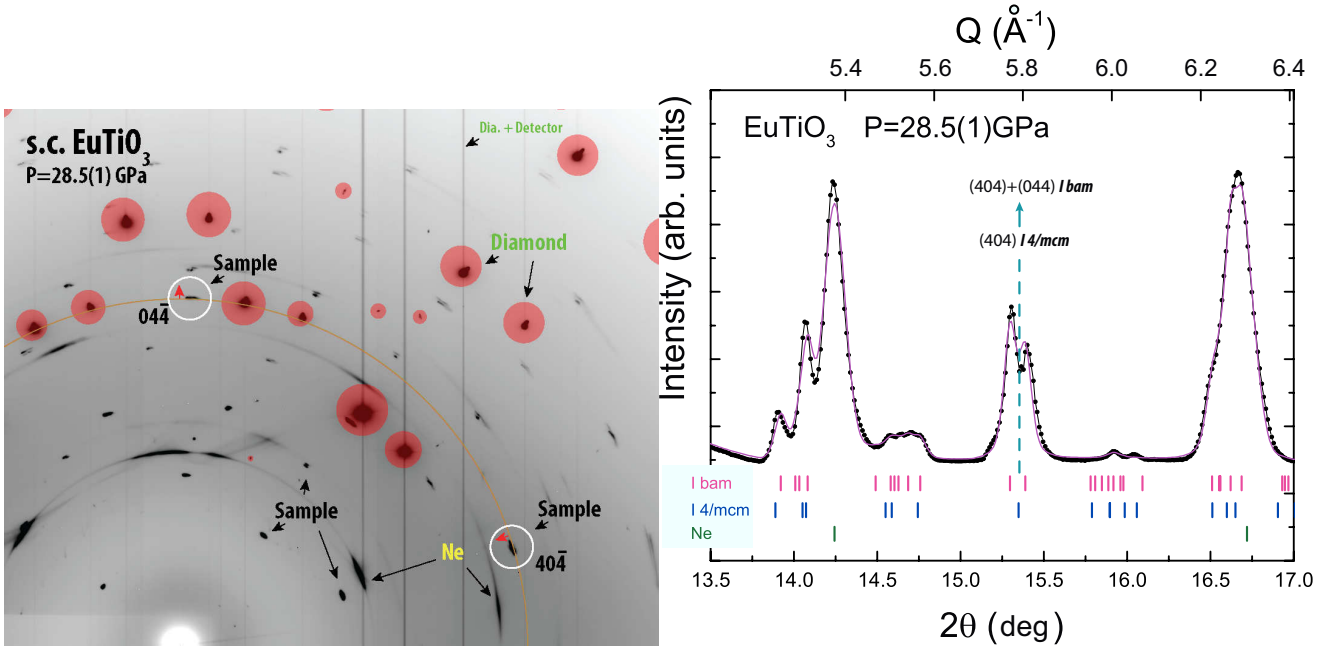

Figure 1: (Left) 2D X-ray diffraction pattern of single crystalline $EuTiO_3$ measured at $28.5(1)$ GPa. Tick marks illustrate signal relevant to the high pressure environment (diamond anvils, Ne pressure medium) and the sample. (Right) An excerpt 1D representation of the same 2D diffraction pattern (black tics) and the Le Bail refinement (pink line). The expected reflection positions are given at the bottom. Splitting of the reflections demonstrated in the 1D pattern on the right corresponds to shift of individual reflections to lower and higher 2θ with respect to the reference orange line indicated by red arrows on the left.

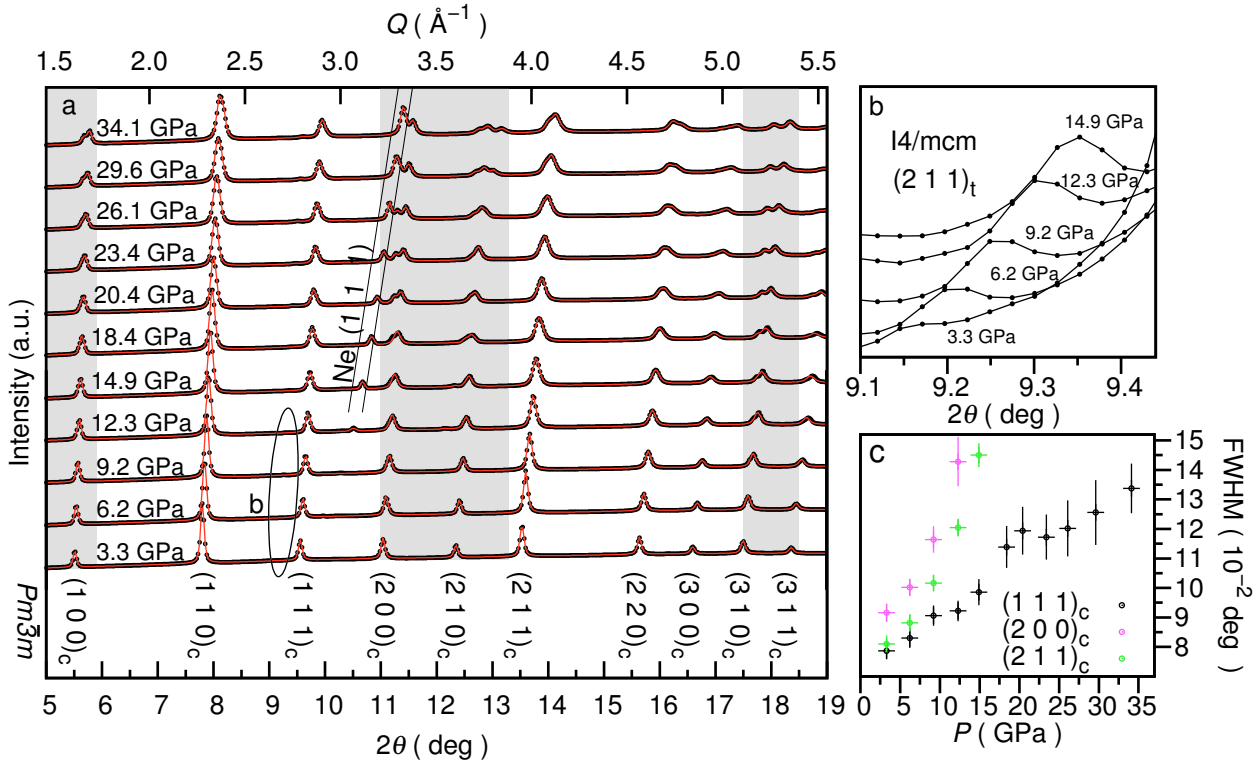

Figure 2: (a) Typical X-ray diffraction patterns obtained by poly-crystalline $EuTiO_3$ between 3 and 34 GPa at room temperature (black data) with Ne as pressure transmitting medium obtained at ID27/ESRF. The pressure dependence of the Ne$(1\ 1\ 1)$ reflection is highlighted. The solid lines (red) show the refinements. The highlighted regions indicate the reflections which clearly split above 10 GPa. The reflection indexing is given in the $Pm\bar{3}m$ space group. (b) The emergence and the pressure dependence of the $(2\ 1\ 1)_t$ reflection in the $I4/mcm$ symmetry above 3.3 GPa. (c) The Full Width at Half Maximum (FWHM) of typical reflections indexed in (a). Typical errorbars are given.

form and do not exhibit significant spikes from large grains of $EuTiO_3$. Typical Le Bail refinements are given in Fig. 2a. A weak reflection, which appears at 12 GPa between the $(1\,1\,1)_c$[40] and the $(2\,0\,0)_c$ reflection, with strong pressure dependence corresponds to the Ne $(1\,1\,1)$ reflection. A gradual emergence as function of pressure of a reflection between 2.5 $Å^{-1}$ and 2.9 $Å^{-1}$ is observed which corresponds to the $(2\,1\,1)_t$ reflection in the $I4/mcm$ space group, see Fig. 2b. For a pressure up to 10 GPa, certain reflections, $e.g.$ $(2\,0\,0)_c$, broaden significantly, see the Full Width at Half Maximum (FWHM) in Fig. 2c. This is well correlated with our observation on twinning and splitting of the reflections in single crystals. However, the situation in polycrystalline samples can be more complicated because of inter-grain micro-strains. Above 10 GPa a clear reflection splitting is observed, see highlighted regions of Fig. 2a. One specific reflection, $(1\,1\,1)_c$, not only does not split even up to 35 GPa but its FWHM shows within the errorbar a linear dependence as function of pressure, see Fig. 2c. Finally, a significant width increase for the $(2\,2\,0)_c$ reflection and reflections with higher Q values is observed upon compression.

Similar X-ray diffraction measurements were carried out using a methanol - ethanol mixture $(4:1)$ as a pressure transmitting medium[31]. The diffractograms below the observed phase transition are essentially the same and the structural phase transition appears at the same pressure range. However, the pressure at which the structural phase transition occurs coincides with the hydrostatic limit of the methanol - ethanol mixture[29], and thus the result obtained at this pressure range cannot be conclusive from this data alone.

C. Electrical resistivity

The electrical resistivity curve measured in this study at ambient pressure on a polycrystalline $EuTiO_3$ sample from the same batch is depicted in Fig. 3a. The electrical resistivity of the sample first decreases between 5 and 30 K and then increases between 40 and 300 K. The electrical resistivity of two characteristic $EuTiO_3$ samples, namely #3 (insulating behavior) and #4 (metallic behavior), taken from Ref. [14] along with the measured concentration of charge carriers is depicted for comparison. From a comparion between the measured and the reference data, a charge carrier density concentration for the polycrystalline sample under study is estimated to be about 10^{18} carriers/cm^3.

D. Nuclear forward scattering

The ^{151}Eu NFS spectrum obtained on a polycrystalline $EuTiO_3$ sample from the same batch at 20 GPa and 20(10) K is shown in Fig. 3b. The spectrum can be unambiguously explained by dynamical scattering that originates in the large nuclear effective thickness of the sample[32]. As in all other spectra we did not observe any quantum beats which could be attributed to magnetic ordering[31].

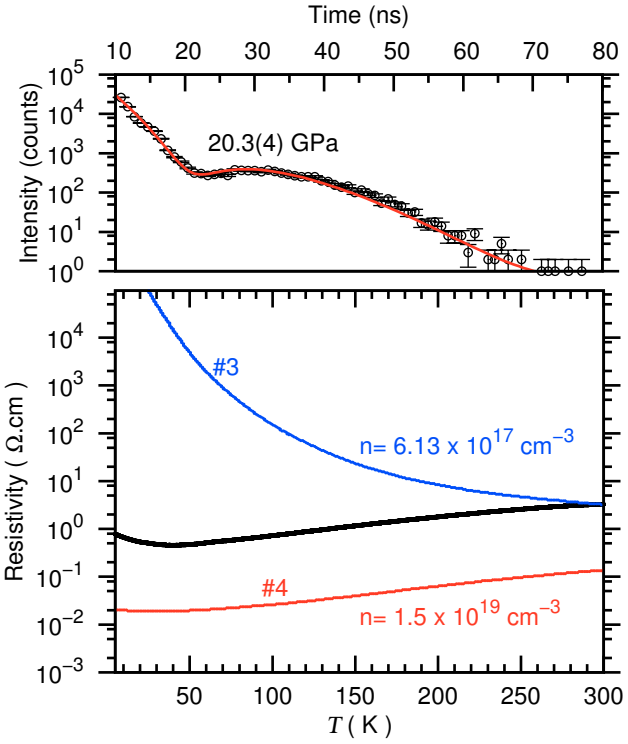

Figure 3: (lower panel) The electrical resistivity of $EuTiO_3$ between 5 and 300 K measured in this study (black ticks) and similar curves (red, blue) obtained in Ref. [14] with the corresponding concentrations of charge carriers. (upper panel) The nuclear forward scattering spectrum obtained on $EuTiO_3$ at 20(10) K and 20GPa (black tics) and a fit of the experimental data using dynamical scattering that originates in the effective thickness of the sample (red line).

IV. DISCUSSION

A. Symmetry analysis and phase diagram at high pressures

Several ambient pressure studies indicate that the space group for the low temperature ground state of $EuTiO_3$ is $I4/mcm$[8–11]. The same $I4/mcm$ space group is expected to be the ground state at high pressure. The appearance of a new reflection between 2.5 $Å^{-1}$ and 2.9 $Å^{-1}$ above 3 GPa which can be indexed as a $(2\,1\,1)_t$ type of reflection in the $I4/mcm$ space group clearly indicates that the system distorts towards a tetragonal symmetry. The lower panel of Fig. 4 shows the lattice parameters ratio evolution. Although the $(2\,1\,1)_t$ type of reflection appears as low as 3 GPa it is at 8(1) GPa that the effect is clearly visible in the lattice parameters ratio measured both on polycrystalline samples and single crystals.

A summary of the high pressure structural phase diagram at room temperature is given in the upper panel of Fig. 4. Notably, above 7 GPa the measured crystals appeared to be twinned and the effects is stronger when the pressure increases. We have verified this effect on several crystals. Thus, twinning seems to be an intrinsic phenomenon in bulk $EuTiO_3$ at high pressures. The transition to the orthorhombic phase above 23 GPa is not reported by Parisiades *et al.*,[20]. This

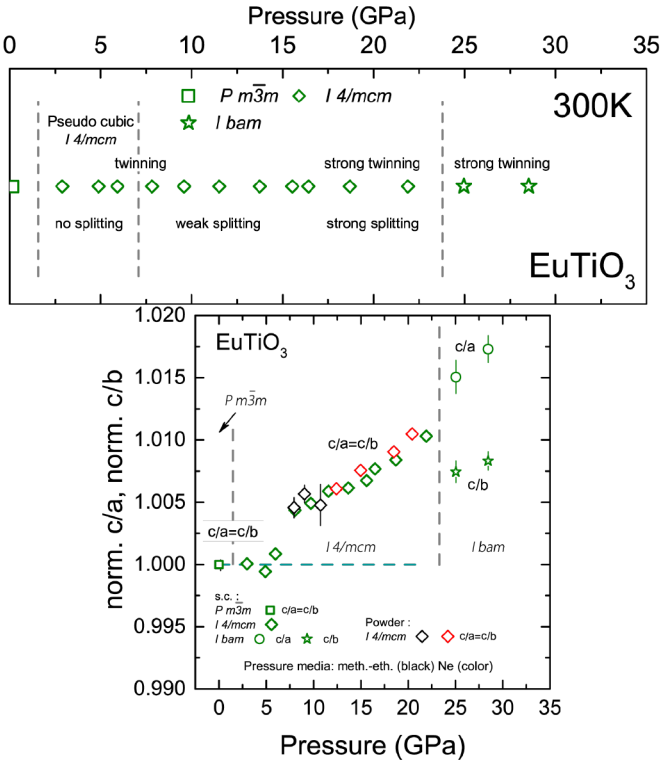

Figure 4: (upper panel) A summary of the phase diagram of $EuTiO_3$ at 300 K up to 30 GPa obtained in this study using single crystalline (s.c.) samples. By the term of weak or strong twinning we indicate the effect of compression on mosaicity and overlapping of the reflections; see text. (lower panel) The normalized lattice parameter ratio (transformed into the original cubic setting) across the structural phase diagram shown in the upper panel. Typical errorbars are given. The dashed lines are guides to the eye.

might stem from various factors, to mention some: the large width of diffraction peaks reported in Ref.[20], the inhomogeneous micro-strain field created in powder aggregated which could stabilize metastable states. In this study higher sensitivity was obtained by means of single crystal data ($i.e.$, narrower diffraction peaks) which shed more light on the phase diagram of $EuTiO_3$ at high pressure.

B. Equation of states and Elasticity

In single crystalline $EuTiO_3$ under externally applied pressure two structural phase transitions take place below 30 GPa. As a result only a descriptive equation of states can be extracted below 30 GPa. In this study an ambient conditions isothermal bulk modulus of 177(3) GPa is obtained in $EuTiO_3$ by fitting the volume - pressure data with a 2nd order Birch - Murnagham equation of states. The obtained value is higher than the adiabatic bulk modulus, 153(4) GPa, obtained by ultrasonic spectroscopy above the lattice instability temperature[15], but a value close to the bulk modulus, 173 GPa, obtained from the room temperature elastic constants measured by Li $et\ al.$,[23] using a similar technique. However, this value is in contrast with the isothermal bulk modulus of $\sim$ 50 GPa extracted from the pressure dependence of the lattice parameter presented by Guguchia $et\ al.$,[33] and is not compatible with a Young modulus of $\sim$ 4 GPa measured by Goian

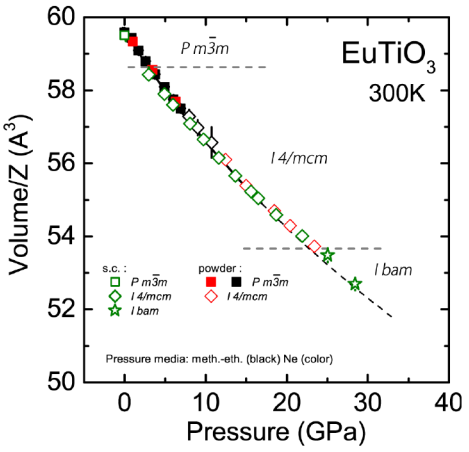

Figure 5: The volume (normalized to formula unit Z; $Z = 1$ for $Pm\bar{3}m$ and $Z = 4$ for $I4/mcm$ and $Ibam$) as function of externally applied pressure in $EuTiO_3$ at 300 K up to 30 GPa obtained in this study by a collection of diffraction data obtained both on single- (s.c.) and poly-crystalline (powder) samples using, as indicated, either Ne or a mixture of methanol-ethanol as a pressure transmitting medium.

$et\ al.$,[13] at room temperature. Though differences between the adiabatic, B_S, and the isothermal, B_T, bulk moduli are expected, the lowest possible B_S value is equal to the isothermal

bulk modulus according to the relation: $B_S = (C_P/C_V)B_T$, where C_P and C_V is the heat capacity at constant pressure and volume, respectively. Significantly lower reported bulk moduli could, thus, be attributed to experimental uncertainties or systematic errors.

C. Analogy between $SrTiO_3$ and $EuTiO_3$

$EuTiO_3$ and $SrTiO_3$ have very similar unit cell volumes and bulk moduli, thus, a direct comparison of their high pressure behaviour could be expected. The transition pressure to the tetragonal phase for $SrTiO_3$ at room temperature is at about 9 GPa[6]. A clear indication of a structural transition towards the $I4/mcm$ space group is detected in $EuTiO_3$ as low as 3 GPa on three samples of different origin, namely, our pre-characterized powder[15], our single crystals [12,24], and the powder of Parisiadis *et al.*, [20]. In this study we moreover show that a second transition to an orthorhombic phase occurs at 23(1) GPa in $EuTiO_3$. If a direct comparison of the high pressure behaviour between $SrTiO_3$ and $EuTiO_3$ is valid, the ratio of transition pressures to the tetragonal symmetry between $SrTiO_3$ and $EuTiO_3$ indicate that a transition to an orthorhombic symmetry is expected to take place in $SrTiO_3$ at around 70 GPa. A current review of the literature pertinent to the high pressure phase diagram of (Sr,Eu)TiO_3 does not report such a transition to the orthorhombic phase [34]. Thus, currently any comparison between the high pressure behaviour of $SrTiO_3$ and $EuTiO_3$ should be done carefully, which seems appropriate, given the difference in electronic configuration, atomic volume and presence of f-shells in $EuTiO_3$.

D. Stoichiometry and disorder

Sagarna *et al.*,[17] suggested that even small oxygen off-stoichiometry might produce an observable amount of Eu(III) which may modify physical properties. However, Kennedy *et al.*,[14] claimed that oxygen vacancies result in negative sign in the Hall coefficient which is consistent with a Ti(IV) to Ti(III) change. In order to clarify the partial population of the Ti $3d$ orbitals expected in the presence of $3d^1$ Ti (III), electrical resistivity measurements were carried out on our polycrystalline samples, see Fig. 3a. The measured resistivity in this study is in the carrier concentration region where a transition from a metallic to an insulating behavior is observed, here at 35 K. This region corresponds to $\sim 10^{18}$ carriers/cm^3. The theoretically expected critical charge carrier concentration for the transition given by the Mott criterion[35] for $EuTiO_3$ is 10^{15} carriers/cm^3, *i.e.*, three order of magnitudes lower than the charge carrier concentration extracted in this study. Such a difference according to Kennedy *et al.*,[14] can be attributed to a significant degree of disorder due to the defect induced random field of potentials.

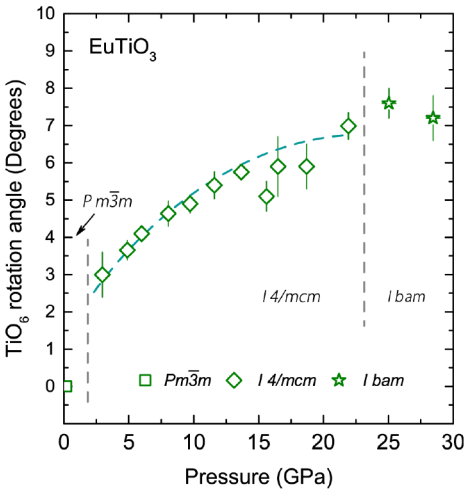

Figure 6: The relative rotation angle of the TiO_6 octahedra up to 30 GPa calculated in the structures identified in this study. The dashed line is a guide for the eyes.

E. Rotation of Oxygen octahedra

The most commonly accepted type of disorder in the perovskite structure is related with the rotation of the corner sharing oxygen octahedra. Parisiades *et al.*,[20] tried to estimate the relative angle for the rotation of such octahedra in $EuTiO_3$, however, the authors had only limited access to structural information. Our data obtained on single crystals allow us to make a step further and shed more light on subtle effects of compression on the structure of $EuTiO_3$. Fig. 6 shows the extracted rotation angle for the TiO_6 octahedra up to 30 GPa. The relative rotation angle in the tetragonal phase ($I4/mcm$ space group) is finite and non negligible even at 3 GPa. The process of TiO_6 rotation stands behind the appearance of the new reflections differentiating the cubic phase of $EuTiO_3$ from the tetragonal one. We observe an increase of the rotation angle with compression. However, the rotation angle seems to approach a constant value in the vicinity of the transformation into the orthorhombic phase. This practically means that the relatively large Eu^{2+} ion compared with the compact TiO_6 framework may accommodate for an external stress by means of Eu-site distortion. In this case the TiO_6 octahedron remains ideal, see table in Supplementary information, thus, the difference between different Ti-O bonds is negligible. This reasoning is additionally supported by our observation of a constant c/a ratio below 8 GPa.

F. Eu valence and magnetism

NFS measurements under high pressure can be useful in order to follow the effect of compression on chemistry and to track valence transitions[36] or magnetic ordering[37]. The experimental conditions of our measurements limited the accessible temperature range for the diamond anvil cell between 20 and 300 K. The obtained NFS data indicate that (i) no magnetic

hyperfine splitting is observed and (ii) Eu exhibits a single valence state up to 20 GPa in the measured temperature range. As the NFS data at 20 GPa and 20 K, see Fig. 3b, do not show any high frequency oscillations, which is the fingerprint of magnetic ordering in NFS[38], the magnetic ordering if present should be below 20 K. Extrapolating linearly the T_N versus pressure observed by Guguchia *et al.*,[33] leads to an expected T_N of about 18 K, thus, a strong increase of T_N between 5.5 and 20 GPa is precluded by our data. As all NFS data do not exhibit the characteristic time pattern (regular beating) with a period of 57 ns, which corresponds to -12 mm/s relative to EuF_3 according to Mössbauer spectroscopy carried out in Ref.[15], the presence of a Eu(III) impurity is also precluded at the detection limit of 1%. Typical signals observed for contrasting examples where mixed valence Eu is observed have been reported *e.g.* in Ref.[36]. Thus, potential oxidation of Eu by aging or applied pressure did not occur in the samples studied herein. Thus, here we show that Eu^{2+} pure $EuTiO_3$ crystallizes in the $I4/mcm$ space group at 20 GPa.

V. CONCLUSION

In summary, we have revisited the structural phase equilibrium both in polycrystalline samples and single crystals of $EuTiO_3$ under externally applied pressure using diffraction of synchrotron radiation at room temperature up to 30 GPa. We reviewed the similarities and the differences of high pressure behavior between $SrTiO_3$ and $EuTiO_3$. We approach the issue of stoichiometry and disorder in $EuTiO_3$ additionally constraining the electronic high pressure phase diagram. We report no magnetic ordering of Eu at 20 GPa and 20 K. Finally we report a previously unknown phase transition of $EuTiO_3$ from the $I4/mcm$ space group to the $Ibam$ space group at about 23 GPa.

Acknowledgments

The Helmholtz Association of German research centers is acknowledged for funding (VH NG-407 "Lattice dynamics in emerging functional materials"). The European Synchrotron Radiation Facility and the Deutsches Elektronen-Synchrotron are acknowledged for provision of synchrotron radiation beam time at ID18, ID27 and P02, respectively. Dr. V. Svitlyk is acknowledged for help during data acquisition at ID27. Dr. M. Manley and Dr. J. Budai are acknowledged for helpful discussions. We thank Dr. A. I. Chumakov and Dr. R. Rüffer for helpful discussions and Mr. J.-P. Celse for technical assistance during the beamtime at ID18. D.B. acknowledges support from the Industrial Partnership Program (IPP-I28) of Foundation for Fundamental Research on Matter (FOM) (The Netherlands) and BASF New Business. R. P. H.: This manuscript has been authored by UT-Battelle, LLC under Contract No. DE-AC05-00OR22725 with the U.S. Department of Energy.

* Electronic address: bessas@esrf.com
† Electronic address: konstantin.glazyrin@desy.de
‡ Present address: European Synchrotron Radiation Facility, F-38043 Grenoble, France.
§ Present address: Technical University of Denmark, Department of Physics, DK-2800 Lyngby, Denmark
¶ Former address: Jülich Centre for Neutron Science, JCNS, and Peter Grünberg Institut PGI, JARA-FIT, Forschungszentrum Jülich GmbH, D-52425 Jülich, Germany

[1] J. Li, S. Li, F. Liu, M. Alim, and G. Chen, J. Mater. Sci. - Mater. Electron. **14**, 483 (2003).
[2] A. B. Kozyrev, T. B. Samoilova, A. A. Golovkov, E. K. Hollmann, D. A. Kalinikos, V. E. Loginov, A. M. Prudan, O. I. Soldatenkov, D. Galt, C. H. Mueller, et al., J. Appl. Phys. **84**, 3326 (1998).
[3] T. R. McGuire, B. E. Argyle, M. W. Shafer, and J. S. Smart, J. Appl. Phys. **34**, 1345 (1963).
[4] P. J. Ryan, J.-W. Kim, T. Birol, P. Thompson, J.-H. Lee, X. Ke, P. S. Normile, E. Karapetrova, P. Schiffer, S. D. Brown, et al., Nat. Commun. **4**, 1334 (2013).
[5] F. W. Lytle, J. Appl. Phys. **35**, 2212 (1964).
[6] M. Guennou, P. Bouvier, J. Kreisel, and D. Machon, Phys. Rev. B **81**, 054115 (2010).
[7] J. Brous, I. Fankuchen, and E. Banks, Acta Cryst. **6**, 67 (1953).
[8] M. Allieta, M. Scavini, L. J. Spalek, V. Scagnoli, H. C. Walker, C. Panagopoulos, S. S. Saxena, T. Katsufuji, and C. Mazzoli, Phys. Rev. B **85**, 184107 (2012).
[9] A. Bussmann-Holder, J. Köhler, R. K. Kremer, and J. M. Law, Phys. Rev. B **83**, 212102 (2011).
[10] J.-W. Kim, P. Thompson, S. Brown, P. S. Normile, J. A. Schlueter, A. Shkabko, A. Weidenkaff, and P. J. Ryan, Phys. Rev. Lett. **110**, 027201 (2013).
[11] J. Köhler, R. Dinnebier, and A. Bussmann-Holder, Phase Transitions **85**, 949 (2012).
[12] D. S. Ellis, H. Uchiyama, S. Tsutsui, K. Sugimoto, K. Kato, D. Ishikawa, and A. Q. R. Baron, Phys. Rev. B **86**, 220301 (2012).
[13] V. Goian, S. Kamba, O. Pacherová, J. Drahokoupil, L. Palatinus, M. Dušek, J. Rohlíček, M. Savinov, F. Laufek, W. Schranz, et al., Phys. Rev. B **86**, 054112 (2012).
[14] B. J. Kennedy, G. Murphy, E. Reynolds, M. Avdeev, H. E. R. Brand, and T. Kolodiazhnyi, J. Phys.: Condens. Matter **26**, 495901 (2014).
[15] D. Bessas, K. Z. Rushchanskii, M. Kachlik, S. Disch, O. Gourdon, J. Bednarcik, K. Maca, I. Sergueev, S. Kamba, M. Ležaić, et al., Phys. Rev. B **88**, 144308 (2013).
[16] L. Sagarna, K. Z. Rushchanskii, A. Maegli, S. Yoon, S. Populoh, A. Shkabko, S. Pokrant, M. Ležaić, R. Waser, and A. Weidenkaff, J. Appl. Phys **114**, 033701 (2013).
[17] L. Sagarna, S. Populoh, A. Shkabko, J. Eilertsen, A. E. Maegli, R. Hauert, M. Schrade, L. Karvonen, and A. Weidenkaff, J. Phys. Chem. C **118**, 7821 (2014).
[18] T. Yamamoto, R. Yoshii, G. Bouilly, Y. Kobayashi, K. Fujita, Y. Kususe, Y. Matsushita, K. Tanaka, and H. Kageyama, Inorg. Chem. **54**, 1501 (2015).
[19] V. S. Zhandun, N. G. Zamkova, and V. I. Zinenko, J. Exp. Theor. Phys. **120**, 103 (2015).
[20] P. Parisiades, E. Liarokapis, J. Köhler, A. Bussmann-Holder, and M. Mezouar, Phys. Rev. B **92**, 064102 (2015).
[21] J. Schiemer, L. J. Spalek, S. S. Saxena, C. Panagopoulos, T. Kat-

sufuji, and M. A. Carpenter, EPL (Europhysics Letters) **109**, 57004 (2015).
[22] L. J. Spalek, S. S. Saxena, C. Panagopoulos, T. Katsufuji, J. A. Schiemer, and M. A. Carpenter, Phys. Rev. B **90**, 054119 (2014).
[23] L. Li, J. R. Morris, M. R. Koehler, Z. Dun, H. Zhou, J. Yan, D. Mandrus, and V. Keppens, Phys. Rev. B **92**, 024109 (2015).
[24] D. S. Ellis, H. Uchiyama, S. Tsutsui, K. Sugimoto, K. Kato, and A. Q. Baron, Physica B **442**, 34 (2014).
[25] C. Prescher and V. B. Prakapenka, High Pressure Res. **35**, 223 (2015).
[26] A. P. Hammersley, S. O. Svensson, M. Hanfland, A. N. Fitch, and D. Hausermann, High Pressure Res. **14**, 235 (1996).
[27] CrysAlis PRO. Rigaku Oxford Diffraction, Yarnton, England.
[28] V. Petříček, M. Dušek, and L. Palatinus, *Jana 2006. The crystallographic computing system.* (2006).
[29] S. Klotz, J.-C. Chervin, P. Munsch, and G. L. Marchand, J. Phys. D: Appl. Phys. **42**, 075413 (2009).
[30] O. Leupold, J. Pollmann, E. Gerdau, H. D. Rüter, G. Faigel, M. Tegze, G. Bortel, R. Rüffer, A. I. Chumakov, and A. Q. R. Baron, EPL **35**, 671 (1996).
[31] Supplementary Material is available.
[32] R. E. Simon, I. Sergueev, J. Persson, C. A. McCammon, F. Hatert, and R. P. Hermann, EPL (Europhysics Letters) **104**, 17006 (2013).
[33] Z. Guguchia, K. Caslin, R. K. Kremer, H. Keller, A. Shengelaya, A. Maisuradze, J. L. B. Jr, J. Köhler, A. Bussmann-Holder, and M.-H. Whangbo, J. Phys.: Condens. Matter **25**, 376002 (2013).
[34] P. Parisiades, F. Saltarelli, E. Liarokapis, J. Köhler, and A. Bussmann-Holder, AIP Advances **6**, 065019 (2016).
[35] P. P. Edwards and M. J. Sienko, Phys. Rev. B **17**, 2575 (1978).
[36] N. M. Souza-Neto, J. Zhao, E. E. Alp, G. Shen, S. V. Sinogeikin, G. Lapertot, and D. Haskel, Phys. Rev. Lett. **109**, 026403 (2012).
[37] I. Sergueev, L. Dubrovinsky, M. Ekholm, O. Y. Vekilova, A. I. Chumakov, M. Zając, V. Potapkin, I. Kantor, S. Bornemann, H. Ebert, et al., Phys. Rev. Lett. **111**, 157601 (2013).
[38] R. Lübbers, M. Pleines, H.-J. Hesse, G. Wortmann, H. Grünsteudel, R. Rüffer, O. Leupold, and J. Zukrowski, Hyperfine Interact. **120-121**, 49 (1999).
[39] Subscript t denotes tetragonal symmetry
[40] Subscript c denotes cubic symmetry